

Stable-RAG: Mitigating Retrieval-Permutation-Induced Hallucinations in Retrieval-Augmented Generation

Qianchi Zhang^{1,2}, Hainan Zhang^{1,2*}, Liang Pang⁴, Hongwei Zheng³, Zhiming Zheng^{1,2},

¹Beijing Advanced Innovation Center for Future Blockchain and Privacy Computing,

²School of Artificial Intelligence, Beihang University, China,

³Beijing Academy of Blockchain and Edge Computing, China,

⁴Institute of Computing Technology, Chinese Academy of Sciences, Beijing, China,

{zhangqianchi, zhanghainan}@buaa.edu.cn

Abstract

Retrieval-Augmented Generation (RAG) has become a key paradigm for reducing factual hallucinations in large language models (LLMs), yet little is known about how the order of retrieved documents affects model behavior. We empirically show that under Top-5 retrieval with the gold document included, LLM answers vary substantially across permutations of the retrieved set, even when the gold document is fixed in the first position. This reveals a previously underexplored sensitivity to retrieval permutations. Although robust RAG methods primarily focus on enhancing LLM robustness to low-quality retrieval and mitigating positional bias to distribute attention fairly over long contexts, neither approach directly addresses permutation sensitivity. In this paper, we propose **Stable-RAG**, which exploits permutation sensitivity estimation to mitigate permutation-induced hallucinations. Stable-RAG runs the generator under multiple retrieval orders, clusters hidden states, and decodes from a cluster-center representation that captures the dominant reasoning pattern. It then uses these reasoning results to align hallucinated outputs toward the correct answer, encouraging the model to produce consistent and accurate predictions across document permutations. Experiments on three QA datasets show that Stable-RAG significantly improves answer accuracy, reasoning consistency and robust generalization across datasets, retrievers, and input lengths compared with baselines.

1 Introduction

Large language models (LLMs) have achieved remarkable performance on language understanding and generation tasks, but still often generate confident yet incorrect statements, known as factual hallucinations (Fan et al., 2024), especially in knowledge-intensive settings (Chen et al., 2022;

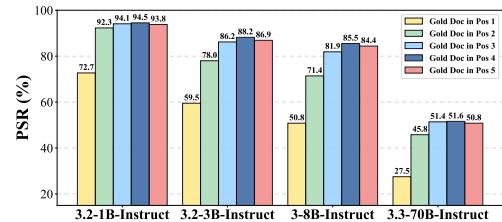


Figure 1: **Perturbation Success Rate (PSR)** on the NQ test set across different LLaMA models. PSR is computed as the proportion of successful document-order perturbations to produce hallucination results among 1000 randomly sampled instances, with the gold document fixed in the different positions. Qwen models’ results can be seen in Appendix C.1.

Huang et al., 2023). Retrieval-Augmented Generation (RAG) (Gao et al., 2023; Lewis et al., 2020) reduces factual hallucinations by grounding model outputs in externally retrieved documents rather than relying only on parametric knowledge, improving factuality, interpretability, and updatability without additional retraining (Zhou et al., 2024).

Despite these benefits, RAG systems are far from hallucination-free. We identify a critical but overlooked vulnerability in existing RAG systems: a strong sensitivity to the order of retrieved documents. When the retrieved content remains exactly the same, including the gold document, merely re-ordering them can lead the model to follow entirely different reasoning paths and produce inconsistent answers, referred to as **Permutation-Induced Hallucinations**. As shown in Figure 1, we retrieve the Top-5 documents (Zhu et al., 2024b; Xu et al., 2024) and place the gold document at different positions, LLM answers vary substantially across retrieval permutations. Even when the gold document is fixed first, models may still ignore it and produce answers that conflict with the evidence. This reveals a previously underexplored sensitivity to retrieval permutations, even for such short contexts shorter than one thousand tokens.

*Corresponding author.

Existing work on RAG robustness mainly focus on retrieval quality and positional bias. The former enhances LLM robustness to low-quality retrieval via uncertainty estimation and adversarial training, such as noise injection (Fang et al., 2024; Yoran et al., 2024) of weak-relevant documents. The latter alleviates attention bias toward specific positions in long contexts, promoting more balanced use of retrieved documents (Zhang et al., 2024c; Wang et al., 2025b). However, these approaches overlook a critical issue: permutation sensitivity is neither caused by weakly relevant documents, because the input documents are the same, nor confined to long-context reasoning tasks, since only the Top-5 documents fall within one thousand tokens.

Instead, permutation sensitivity stems from structural instability in the internal reasoning dynamics of LLMs. As model depth increases, document permutations induce a growing number of distinct reasoning trajectories, leading to more frequent branching and a higher risk of hallucinations or unreliable outputs. As shown in Figure 2, we measure the average number of clusters obtained via spectral clustering over document-permuted representations across different LLM layers on the NQ and HotpotQA datasets. The results indicate that reasoning trajectories in shallow layers are relatively concentrated, while divergence emerges in the middle layers and becomes more pronounced in higher layers. Furthermore, sensitive samples (i.e., 10+) exhibit substantially greater divergence than non-sensitive ones (i.e., 1-2), with this effect primarily localized to the higher layers. These findings highlight the importance of mitigating permutation sensitivity, enabling LLMs to produce stable and accurate outputs regardless of the ordering of retrieved documents, which is critical for improving the robustness of RAG systems.

In this paper, we introduce **Stable-RAG** that explicitly leverages permutation sensitivity estimation to mitigate the permutation-induced hallucinations. Specifically, we apply spectral clustering to the last token hidden states of the final layer before response generation, across all document permutations to identify dominant reasoning clusters. For each cluster, we select a representative hidden state and decode it to obtain candidate answers, thereby capturing the model’s core reasoning modes. Then, we perform cross-cluster consistency alignment over these candidates, encouraging the model to prioritize semantically consistent and factually correct answers across different document orders. This

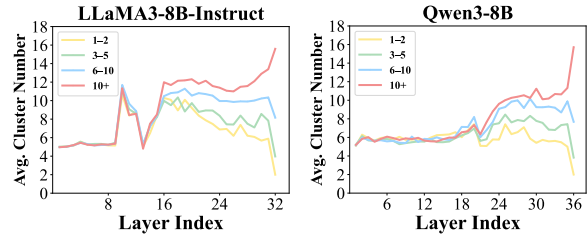


Figure 2: Hidden-state clustering behaviors across layers for LLaMA3-8B-Instruct on the NQ train set with DPR retriever and Qwen3-8B on the HotpotQA train set with Contriever retriever, using 1,000 random sampled instances. Different colored lines indicate the number of clusters of final reasoning states produced by the LLM under all $5! (= 120)$ permutations of the Top-5 retrieved documents (e.g., the green line indicates 3–5 cluster states). Other scales are reported in Appendix C.2.

cluster-based alignment substantially reduces the uncertainty induced by order perturbations and improves the robustness of RAG at its root.

Experiments on three QA datasets demonstrate that Stable-RAG significantly improves answer accuracy, reasoning consistency and robust generalization across datasets, retrievers, and input lengths compared with strong baselines.

Our main contributions are as follows:

- We find that RAG systems are highly sensitive to document order, leading to inconsistent reasoning. We analyze this permutation sensitivity via layer-wise hidden state clustering, showing divergence in reasoning trajectories across layers.
- We propose Stable-RAG, which mitigates permutation-induced hallucinations using cluster-based decoding and alignment, achieving model-agnostic stable reasoning.
- Across three QA datasets, Stable-RAG outperforms strong baselines in accuracy and reasoning consistency and generalizes across datasets, retrievers, and input lengths.

2 Related Work

RAG mitigates factual hallucinations in LLMs for knowledge-intensive tasks by providing explicit evidence from external documents (Lewis et al., 2020; Fan et al., 2024; Chen et al., 2022). Prior work on improving the robustness of RAG systems has primarily focused on enhancing retrieval quality (Wang et al., 2025a; Xu et al., 2024) or strengthening the generator’s robustness. For instance,

Selective-Context (Li et al., 2023), EXIT (Hwang et al., 2025), and AdaComp (Zhang et al., 2024b) apply noise filtering to boost generation accuracy; RetRobust (Yoran et al., 2024) and RAAT (Fang et al., 2024) expose the model to retrieval noise or irrelevant documents during training, enhancing robustness. However, these methods generally assume a stable document order and do not systematically assess its impact on reasoning. Although ATM (Zhu et al., 2024a) considers order perturbations, it does not explicitly model reasoning trajectories across permutations, and thus cannot ensure consistency.

Additionally, another line of research focuses on positional bias in long-context scenarios. Most LLMs use relative positional encodings (Peysakhovich and Lerer, 2023), such as RoPE (Su et al., 2024) or ALiBi (Press et al., 2021), which introduce systematic biases: early tokens receive excessive attention due to attention sinks (Xiao et al.; Gu et al.), while long-range decay favors recent tokens. Prior work mitigates these issues by modifying positional encodings (Zhang et al., 2024c; Chen et al., 2024; Lin et al., 2024), adjusting causal masks, reweighting attention or hidden states (Hsieh et al., 2024), or using Pos2Distill (Wang et al., 2025b) to distill knowledge from advantageous to less favorable positions to promote fair attention across tokens. However, these methods mainly target long contexts or large document sets and do not explicitly address reasoning inconsistencies induced by different permutations of the same retrieved document set.

3 Preliminary Study

3.1 Problem Formulation

Given a query q and its retrieved document set $\mathcal{S} = \{d_1, d_2, \dots, d_n\}$, the goal is to ensure that the model f_θ produces consistent outputs across different document orderings. Let $\text{Perm}(\mathcal{S})$ denote all possible permutations of \mathcal{S} . For any two permutations $\pi_1, \pi_2 \in \text{Perm}(\mathcal{S})$, the model’s outputs should be as similar as possible:

$$f_\theta(q, \pi_1) \approx f_\theta(q, \pi_2).$$

In this task, the model is expected to produce consistent answers regardless of the document order.

3.2 Permutation Sensitivity Estimation

Recent work (Liang et al., 2025; Lee et al., 2025) exploits hidden states to uncover latent reasoning

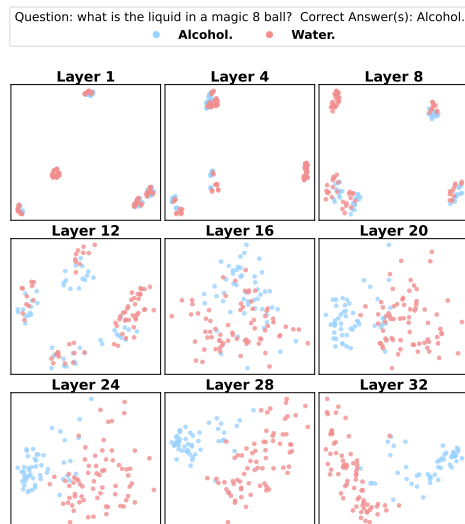


Figure 3: The layer-wise visualization of case study from the NQ train set on LLaMA-3-8B-Instruct. Each point corresponds to a document order, and its color represents the model’s final answer.

trajectories, often as indicators of generative uncertainty. Accordingly, we propose to quantify model generation uncertainty via spectral clustering of hidden states. In this section, we validate the feasibility of spectral clustering algorithm through both layer-wise visualization and quantitative analysis.

Layer-wise Visualization. For each question, we permute the Top-5 documents to generate $5! = 120$ orders and extract the hidden states of the last token from each layer before response generation. Representative layers are then projected to two dimensions via PCA for visualization, as shown in Figure 3. We observe that hidden states in shallow layers form mixed clusters with points corresponding to different answers interleaved, while in deeper layers the clusters become increasingly well-separated and points with the same answer clearly group together. This indicates that variations in document order induce distinct reasoning trajectories, which manifest as progressively separable clusters in hidden state space, reflecting the model’s internal reasoning patterns. More results are presented in Appendix C.3.

Quantitative Analysis of Clustering. To assess each cluster’s reasoning performance, we select the hidden state closest to the cluster center, decode it as a representative answer of the cluster, and match this answer with the real reasoning answers of all hidden states in the same cluster to compute overall Precision, Recall, and F1 scores. As

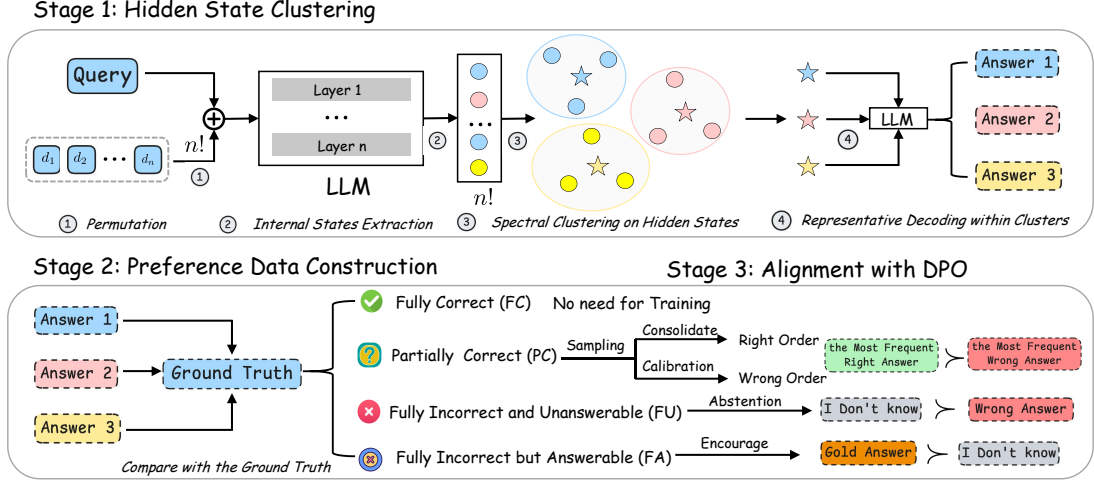


Figure 4: Overall framework of our Stable-RAG.

| Model | Layer | Precision | Recall | F1 |
|--------------------|-------|-----------|--------|------|
| QWEN3-8B | 8 | 78.1 | 79.3 | 77.9 |
| | 16 | 79.9 | 81.3 | 79.6 |
| | 24 | 86.8 | 87.5 | 86.6 |
| | 36 | 87.8 | 88.4 | 87.6 |
| LLAMA3-8B-INSTRUCT | 8 | 69.2 | 71.8 | 69.3 |
| | 16 | 81.4 | 82.5 | 81.3 |
| | 24 | 82.3 | 83.7 | 82.2 |
| | 32 | 84.1 | 85.2 | 83.9 |

Table 1: Clustering performance (%) of hidden states across different layers for Qwen3-8B and LLaMA3-8B-Instruct on the NQ train set using DPR retriever, evaluated on 10,000 randomly sampled instances.

shown in Table 1, clustering metrics improve with network depth, indicating that hidden states for different answers become more separable in deeper layers. Notably, the clustering performance is already satisfactory for practical use, with F1 scores of 83.9 using LLaMA3 and 87.6 using Qwen3, respectively. Thus, we use the final layer hidden states for spectral clustering in our method.

4 Methodology

Overview. Our method comprises three stages: hidden state clustering, preference data construction and alignment with DPO, as shown in Figure 4. For each permutation, we extract the last token hidden state of the final layer before response generation, capturing the model’s reasoning states. Spectral clustering is then applied to uncover latent reasoning modes, and representative states from each cluster are decoded. By aligning hidden states across permutations, our approach improves generation consistency across different retrieval orders.

4.1 Hidden State Clustering

Internal States Extraction. For each query q and its retrieved document set $\mathcal{S} = \{d_1, d_2, \dots, d_n\}$, we enumerate all permutations of the documents and run the model for each permutation. Let $i \in \{1, \dots, N\}$ denote the permutation index, where $N = n!$. To reduce computational cost, we extract only the last token hidden state of the final layer before response generation, $h^{(i)} \in \mathbb{R}^d$. Prior work (Azaria and Mitchell, 2023; Ni et al., 2025) has shown that this hidden state sufficiently captures the model’s perception of its knowledge boundaries. We organize all hidden states into a matrix H :

$$H = [h^{(1)}, h^{(2)}, \dots, h^{(N)}]^\top \in \mathbb{R}^{N \times d},$$

which represents the distribution of the model’s final reasoning states across document permutations.

Spectral Clustering on Hidden States. To determine the number of clusters adaptively and capture the global structure of the hidden state space, we apply spectral clustering (Ng et al., 2001) to H , where each cluster corresponds to a latent reasoning mode (Lee et al., 2025). We compute the similarity between each pair of hidden states $h^{(i)}$ and $h^{(j)}$ using the exponential of the cosine distance:

$$A_{ij} = \exp\left(-\frac{1 - \frac{h^{(i)} \cdot h^{(j)}}{\|h^{(i)}\| \|h^{(j)}\|}}{\sigma}\right),$$

where σ is a hyperparameter controlling sensitivity. Here, $A \in \mathbb{R}^{N \times N}$ denotes the weighted adjacency matrix of all N hidden states.

The normalized graph Laplacian L is then constructed as

$$D = \text{diag}\left(\sum_{j=1}^N A_{ij}\right), \quad L = I - D^{-1/2}AD^{-1/2},$$

where D is the degree matrix, with each diagonal entry D_{ii} representing the sum of edge weights connected to the i -th hidden state (treated as a graph node), and I is the identity matrix.

The number of clusters K is determined adaptively via the eigengap of L . Let $\lambda_1 \leq \dots \leq \lambda_N$ be the eigenvalues of L , and define the consecutive gaps $\text{gap}_i = \lambda_{i+1} - \lambda_i$ between each pair of adjacent eigenvalues. The number of clusters is then set as $K = \max(2, (\arg \max_i \text{gap}_i) + 1)$ to ensure clear separation between latent reasoning modes. Once K is determined, we obtain normalized spectral embeddings for all hidden states and assign each $h^{(i)}$ to one of the clusters C_1, C_2, \dots, C_K . See more details in Appendix B.

Representative Decoding within Clusters. Within each cluster C_k , we identify a representative hidden state through centroid-based sampling. The cluster centroid is computed as:

$$\mu_k = \frac{1}{|C_k|} \sum_{h^{(i)} \in C_k} h^{(i)}.$$

We select the representative hidden state:

$$h^{(r_k)} = \arg \min_{h^{(i)} \in C_k} \|h^{(i)} - \mu_k\|_2.$$

Only the representative hidden states selected within each cluster $\{h^{(r_1)}, h^{(r_2)}, \dots, h^{(r_K)}\}$ are decoded into textual answers, reducing the number of runs from $N = n!$ to K and substantially lowering computational and annotation overhead.

Exhaustive Full-Permutation Decoding. We study an exhaustive permutation decoding setting in which the model is evaluated under all ($N = n!$) permutations of retrieved documents. While this fully characterizes permutation-induced output variability, it is computationally and annotationally prohibitive at scale. We therefore use it only as a reference to assess the efficiency gains of our representative decoding strategy.

4.2 Preference Data Construction

Targets. Our goal is to build a robust RAG system. When the model cannot answer, it is encouraged to abstain to suppress hallucinations. When

an answer is available, the output should remain consistent regardless of document order, reducing permutation sensitivity.

Data Construction Procedure. We construct preference data $\mathcal{P} = (x, y_w, y_l)$ for training. For each query q with its retrieved documents set $\mathcal{S} = \{d_1, d_2, \dots, d_n\}$, the input x is formed by concatenating q with a specific document permutation π . Model outputs are obtained via representative decoding of hidden-state clusters induced by document permutations. Each instance is then compared with the ground truth and categorized into the following four types: **FC (Fully Correct)**: the base model produces correct answers under all document permutations. Such instances are stable and excluded from training. **PC (Partially Correct)**: the base model produces both correct and incorrect answers across permutations. Two representative outputs are sampled: y_w is the most frequent right answer to consolidate correct predictions, and y_l is the most frequent wrong answer for calibration. **FU (Fully Incorrect and Unanswerable)**: the base model answers incorrectly under all permutations and no gold answers exist in the documents. y_w is set to “*I don’t know*” to encourage abstention, and y_l is the most frequent wrong answer. **FA (Fully Incorrect but Answerable)**: the base model answers incorrectly under all permutations but a gold answer exists in the documents. y_w is set to the gold answer to encourage correct prediction, and y_l is “*I don’t know*”.

4.3 Alignment with DPO

We employ Direct Preference Optimization (DPO) (Rafailov et al., 2023) to train the base model on the constructed preference tuples. For each tuple (x, y_w, y_l) , DPO maximizes the likelihood of the preferred answer y_w over the less preferred y_l :

$$\mathcal{L}_{\text{DPO}} = -E_{(x, y_w, y_l) \sim \mathcal{D}} \left[\log \sigma \left(\beta \log \frac{\pi_{\theta}(y_w | x)}{\pi_{\text{ref}}(y_w | x)} - \beta \log \frac{\pi_{\theta}(y_l | x)}{\pi_{\text{ref}}(y_l | x)} \right) \right],$$

where θ denotes the model parameters, σ is the sigmoid function, and β is a scaling hyperparameter controlling the sharpness of preference. The model policy π_{θ} is initialized using the base reference policy π_{ref} .

| Method | NQ | | | | TriviaQA | | | | HotpotQA | | | | Average | |
|--------------------------------|--------------|--------------|--------------|--------------|--------------|--------------|--------------|--------------|--------------|--------------|--------------|--------------|--------------|--------------|
| | Contriever | | DPR | | Contriever | | DPR | | Contriever | | DPR | | SubEM | F1 |
| | SubEM | F1 | | |
| LLAMA3-8B-INSTRUCT | | | | | | | | | | | | | | |
| Direct Generation | 25.18 | 29.11 | 25.18 | 29.11 | 55.92 | 58.95 | 55.92 | 58.95 | 21.39 | 22.87 | 21.39 | 22.87 | 34.16 | 36.98 |
| Vanilla RAG | 40.75 | 42.82 | 45.81 | 47.80 | 63.89 | 65.43 | 67.12 | 68.61 | 30.73 | 34.08 | 25.66 | 28.22 | 45.66 | 47.83 |
| Vanilla SFT | 42.10 | 44.78 | 46.20 | 49.44 | 55.52 | 51.40 | 57.10 | 52.51 | 27.25 | 31.58 | 24.63 | 29.85 | 42.13 | 43.26 |
| RetRoBust | 41.82 | 44.26 | 48.70 | 49.29 | 64.85 | 66.72 | 68.67 | 70.42 | 31.46 | 35.34 | 26.96 | 30.36 | 47.08 | 49.40 |
| ATM | 43.75 | 44.88 | 49.78 | 50.19 | 66.37 | 67.12 | 70.12 | 70.35 | 34.36 | 36.97 | 28.55 | 29.31 | 48.82 | 49.80 |
| RAAT | 42.33 | 43.85 | 49.12 | 49.85 | 65.58 | 66.94 | 68.03 | 69.12 | 33.58 | 36.12 | 26.35 | 28.79 | 47.50 | 49.11 |
| Pos2Distill | 44.58 | 43.12 | 49.25 | 48.37 | 64.13 | 65.78 | 66.57 | 68.12 | 32.73 | 35.79 | 26.45 | 28.91 | 47.29 | 48.35 |
| Ms-PoE | 40.32 | 42.49 | 45.58 | 47.53 | 64.21 | 66.14 | 66.48 | 67.73 | 30.17 | 33.65 | 26.12 | 28.57 | 45.48 | 47.69 |
| Stable-RAG (Ours) | 48.14 | 45.80 | 52.02 | 50.72 | 72.05 | 71.56 | 73.43 | 73.76 | 38.91 | 39.87 | 29.48 | 31.68 | 52.34 | 52.23 |
| Stable-RAG [*] (Ours) | 48.75 | 46.58 | 52.88 | 51.78 | 72.13 | 71.89 | 74.01 | 74.12 | 39.12 | 40.16 | 30.41 | 32.12 | 52.88 | 52.78 |
| QWEN3-8B | | | | | | | | | | | | | | |
| Naive Generation | 21.94 | 24.07 | 21.94 | 24.07 | 45.77 | 48.16 | 45.77 | 48.16 | 19.54 | 24.86 | 19.54 | 24.86 | 29.08 | 32.36 |
| Vanilla RAG | 44.65 | 45.34 | 50.55 | 50.67 | 64.35 | 66.29 | 69.62 | 71.03 | 33.14 | 38.66 | 26.17 | 31.33 | 48.08 | 50.55 |
| Vanilla SFT | 41.41 | 45.05 | 45.60 | 49.19 | 51.87 | 47.62 | 54.46 | 50.17 | 28.36 | 34.15 | 25.35 | 29.77 | 41.18 | 42.66 |
| RetRoBust | 43.10 | 44.99 | 49.50 | 50.81 | 63.49 | 65.39 | 69.12 | 70.33 | 32.77 | 39.39 | 26.83 | 33.06 | 47.47 | 50.66 |
| ATM | 45.47 | 45.86 | 50.94 | 51.03 | 64.78 | 66.57 | 70.06 | 71.67 | 35.12 | 40.69 | 29.07 | 33.43 | 49.24 | 51.54 |
| RAAT | 45.13 | 45.87 | 50.12 | 50.03 | 63.12 | 65.17 | 68.54 | 69.88 | 33.54 | 39.06 | 27.21 | 33.75 | 47.94 | 50.63 |
| Pos2Distill | 44.89 | 45.52 | 50.71 | 50.93 | 64.95 | 66.81 | 69.87 | 71.35 | 33.72 | 39.11 | 26.53 | 31.88 | 48.45 | 50.93 |
| Ms-PoE | 44.39 | 45.12 | 50.04 | 50.08 | 64.88 | 66.72 | 69.03 | 70.84 | 32.98 | 38.21 | 25.93 | 31.02 | 47.88 | 50.33 |
| Stable-RAG (Ours) | 46.12 | 46.79 | 51.69 | 51.78 | 66.58 | 68.13 | 71.32 | 72.89 | 35.73 | 41.78 | 30.15 | 33.26 | 50.27 | 52.44 |
| Stable-RAG [*] (Ours) | 46.94 | 47.13 | 52.12 | 52.38 | 67.11 | 68.79 | 71.74 | 73.40 | 36.89 | 42.94 | 31.77 | 35.78 | 51.10 | 53.40 |

Table 2: Main results (%) on three QA benchmarks using two retrievers. ♣ denotes our method trained on exhaustive full-permutation decoding.

5 Experiments

5.1 Experiments Setup

Datasets. We evaluate our method on three QA benchmark datasets, including (1) Open-Domain QA, represented by NaturalQuestions (NQ) (Kwiatkowski et al., 2019) and TriviaQA (Joshi et al., 2017); (2) Multi-Hop QA, represented by HotpotQA (Yang et al., 2018). Dataset statistics are provided in Appendix A.1.

Evaluation Metrics. Since answer style mismatch may cause additional variance, we follow prior work (Zhu et al., 2024a; Peng et al., 2025; Zhang et al., 2025) and adopt Substring Exact Match (**SubEM**) and **F1** for evaluation. SubEM checks whether the gold answer appears as a substring in the prediction, while F1 measures token-level overlap with the reference.

Baselines. We compare our method with the following baseline strategies on the same test set. Vanilla methods include *Direct Generation*, *Vanilla RAG* (Lewis et al., 2020), and *Vanilla SFT* (Zhang et al., 2024a). Robust RAG methods include *RetRobust* (Yoran et al., 2024), *ATM* (Zhu et al., 2024a), and *RAAT* (Fang et al., 2024). Positional Bias methods include *Pos2Distill* (Wang et al., 2025b) and *Ms-PoE* (Zhang et al., 2024c). The details of these baselines are presented in Appendix A.2.

Implementation Details. We use LLaMA3-8B-Instruct (Dubey et al., 2024) and Qwen3-8B (Yang et al., 2025) as backbone models for experiments.

To ensure high and consistent evaluation quality (Cuconasu et al., 2024) and further assess the stability of our method under different retrieval settings, we follow prior work (Zhu et al., 2024b; Xu et al., 2024; Li et al., 2024) and use the same Top-5 Wikipedia passages retrieved by DPR (Karpukhin et al., 2020) and Contriever-MS MARCO (Izacard et al., 2021) for all baselines and our method. Additional implementation details are provided in Appendix A.3.

5.2 Main Results

We conduct a comprehensive comparison of Stable-RAG against all the baseline methods, as shown in Table 2. The results indicate the following: (i) **Overall performance.** Stable-RAG consistently achieves the best overall performance across all the datasets with both Contriever and DPR retrievers, outperforming all baselines; (ii) **Effectiveness on complex reasoning.** Stable-RAG consistently improves performance on both single-hop and multi-hop QA tasks, demonstrating its ability to stabilize intermediate reasoning for complex questions. (iii) **Model generalization.** Stable-RAG performs robustly across backbone models, indicating model-agnostic generalization.

5.3 Further Analysis

Ablation Study. We conduct an ablation study to assess the contribution of each component in Stable-RAG, as shown in Table 3. Removing any component consistently degrades performance, demonstrating that all components are essential.

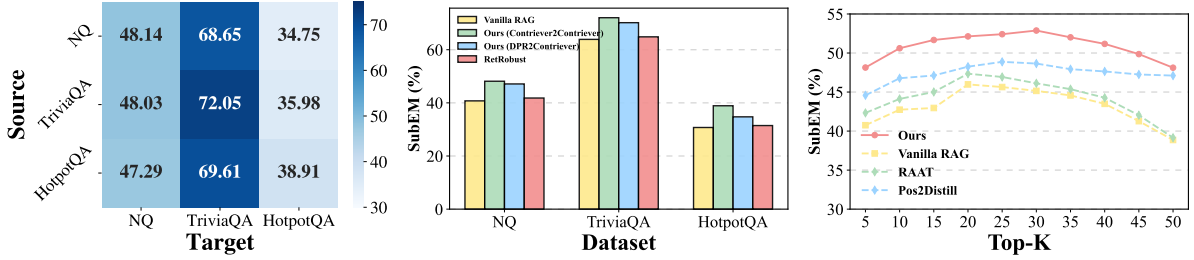


Figure 5: **(Left)** *Cross-Dataset Generalization*. We evaluate on three test sets with the Contriever retriever using SubEM. **(Middle)** *Cross-Retriever Transferability*. **(Right)** *Cross-Top-K Robustness*. We evaluate on the NQ test set with the Contriever retriever. All experiments are conducted on LLaMA3-8B-Instruct.

| Index | component | | | Dataset | | | Average | AR |
|-------------|-----------|----|----|--------------|--------------|--------------|--------------|-------------|
| | PC | FA | FU | NQ | TriviaQA | HotpotQA | | |
| (a) | ✗ | ✓ | ✓ | 37.62 | 61.37 | 28.54 | 42.51 | 35.1 |
| (b) | ✓ | ✗ | ✗ | <u>47.17</u> | <u>71.28</u> | 37.44 | 51.96 | 0.0 |
| (c) | ✓ | ✗ | ✓ | 46.73 | 70.14 | 35.75 | 50.87 | 17.3 |
| (d) | ✓ | ✓ | ✗ | 46.70 | 70.69 | 38.93 | <u>52.11</u> | 0.5 |
| Ours | ✓ | ✓ | ✓ | 48.14 | 72.05 | <u>38.91</u> | 53.03 | <u>21.8</u> |

Table 3: Ablation results (%) on LLaMA3-8B-Instruct with the Contriever retriever measured by SubEM. **AR**(Abstention Rate) denotes the proportion of abstentions on 1,000 randomly sampled questions from three datasets when no retrieval evidence is available and the base model cannot answer. Higher AR indicates better awareness of model limitations and evidence availability. Best and second-best results are bolded and underlined, respectively.

In particular, excluding the *PC* component (Index a) causes significant drops across datasets, indicating the importance of partially correct signals for stabilizing reasoning. Removing *FA* (Index c) mainly impacts overall performance, while removing *FU* (Index b,d) sharply reduces the abstention rate, underscoring its role in handling unanswerable or hallucinated cases. Overall, Stable-RAG achieves the best trade-off between performance and abstention.

Comparison with Standard DPO. To isolate the effect of the order-stability mechanism, we compare Stable-RAG with standard DPO using the same base model and optimization strategy, differing only in whether reasoning consistency across document orders is enforced. In standard DPO, the model is trained to prefer the gold answer when evidence is available over other wrong answers obtained via sampling, or “*I don’t know*” when the query is unanswerable. Results in Table 4 demonstrate that adding the order-stability constraint consistently improves RAG performance across datasets and retrievers without modifying the preference optimization framework.

| Method | NQ | | TriviaQA | | HotpotQA | |
|--------------|--------------|--------------|--------------|--------------|--------------|--------------|
| | Contriever | DPR | Contriever | DPR | Contriever | DPR |
| Standard DPO | 44.76 | 50.88 | 68.03 | 71.67 | 35.96 | 30.43 |
| Ours | 48.14 | 52.02 | 72.04 | 73.43 | 38.91 | 29.48 |

Table 4: SubEM results (%) between our method and Standard DPO using LLaMA3-8B-Instruct.

Cross-Dataset Generalization. We further evaluate the transferability of Stable-RAG across different data distributions. As shown in Figure 5 (Left), permutation-sensitivity patterns are learned on an in-domain dataset and directly applied to multiple out-of-distribution datasets to assess cross-dataset generalization. Experimental results demonstrate that Stable-RAG exhibits robust transfer across tasks and knowledge domains, consistently outperforming the best baseline regardless of the source–target dataset combination, and achieving stable improvements in answer consistency.

Cross-Retriever Transferability. We further evaluate the model’s transferability by training on the DPR retriever and evaluating on the Contriever retriever. Figure 5 (Middle) shows that the model maintains stable performance under cross-retriever settings, demonstrating strong transferability to different retrieval methods. Additionally, the results of training on the Contriever retriever and evaluating on the DPR retriever are shown in Appendix C.4.

Cross-Top-K Robustness. We train the model under a Top-5 setting and evaluate its performance on contexts retrieved with different Top-K values. Experimental results in Figure 5 (Right) show that the model maintains stable performance across various Top-K configurations and achieves significant improvements over corresponding baselines, demonstrating strong generalization when handling different numbers of candidate documents.

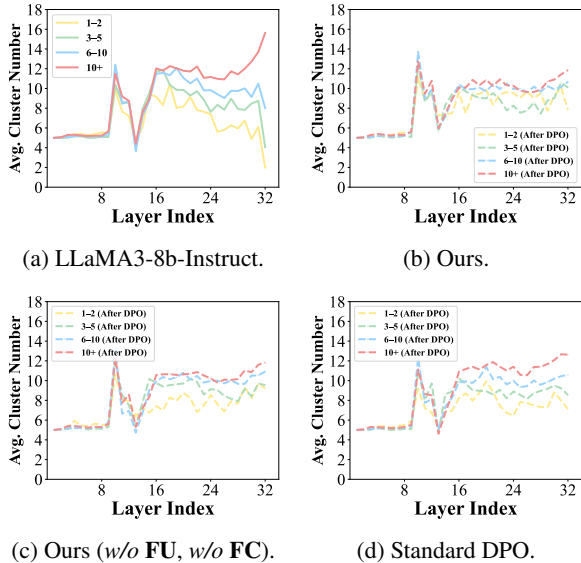


Figure 6: Comparison of internal model behaviors across Base Model (a), Ours (b), one variant of Ours (c), and Standard DPO (d) on a random subset of 500 samples from the NQ test set with Contriever retriever.

Effect of Training Data Size. As shown in Figure 7, we analyze the effect of training sample size on learning permutation sensitivity. Performance improves steadily with more data and saturates beyond 15k samples, indicating relatively small datasets suffice to capture core permutation-sensitivity patterns. However, with very limited data (e.g., 1k), performance drops markedly, reflecting difficulty in modeling fine-grained order differences. Given this trade-off, we adopt 15k samples as default, since gains over 20k do not justify the added computational cost.

Internal Model Behaviors after DPO. We label samples by their sensitivity according to the Base Model and exam hidden-state clustering after training. Figure 6b shows our method reduces clusters for high-sensitivity samples, keeps medium-sensitivity samples stable, and slightly increases low-sensitivity clusters. Figure 6c shows training on sensitive samples only, and Figure 6d shows standard DPO results. We can see that the increased clusters mainly stems from DPO-induced answer diversity rather than direct training on sensitive samples. For instance, for the same query "when was the cat and mouse act introduced?" and order, the response changes from "1913." to "introduced in April 1913." after DPO. Additional examples are in the open-source repository. Overall, our method stabilizes high-sensitivity representations while preserving diversity for less sensitive samples.

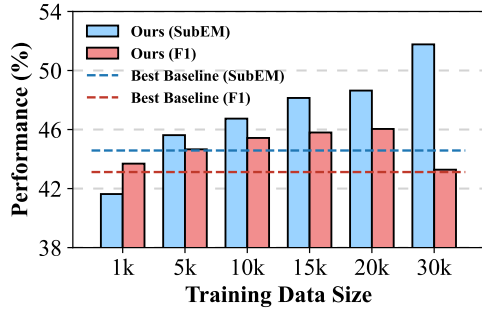


Figure 7: Effect of training sample size on LLaMA3-8B-Instruct with Contriever retriever on NQ dataset.

| Method | Position of Gold Document | | | | |
|-------------|---------------------------|-------------|-------------|-------------|-------------|
| | in Pos 1 | in Pos 2 | in Pos 3 | in Pos 4 | in Pos 5 |
| Vanilla RAG | 50.8 | 71.4 | 81.9 | 85.5 | 84.4 |
| Vanilla SFT | 47.2 | 66.2 | 74.8 | 80.0 | 82.6 |
| RetRobust | 35.5 | 75.5 | 85.3 | 88.6 | 88.9 |
| ATM | 33.7 | 64.2 | 71.8 | 77.4 | 77.8 |
| Pos2Distill | 29.5 | 55.8 | 69.4 | 72.8 | 73.2 |
| Ms-PoE | 31.4 | 63.8 | 72.1 | 73.9 | 74.3 |
| Ours | 28.3 | 54.7 | 67.3 | 72.6 | 73.0 |

Table 5: PSR (%) on the NQ test set with DPR retriever across different document positions, same as Figure 1.

External Positional Robustness after DPO.

Following prior settings, we evaluate PSR on 1,000 randomly sampled instances by inserting the gold document at varying positions in the retrieved context to assess external positional robustness. As shown in Table 5, our method consistently achieves lower PSR across all positions than the baselines, indicating reduced sensitivity to document ordering and improved external robustness under positional perturbations. Experiments in Appendix C.5 further confirms our method’s top performance under both original and shuffled document orders.

6 Conclusion

We identify an underexplored vulnerability in RAG: LLMs are highly sensitive to document order, producing divergent reasoning and inconsistent or hallucinatory outputs from identical evidence. Layer-wise analysis traces this instability to the model’s middle and higher layers. We propose Stable-RAG, which reduces permutation-induced uncertainty by clustering permuted hidden states and aligning reasoning modes via DPO optimization. Experiments across multiple QA benchmarks show consistent gains in accuracy, reasoning stability, and strong transferability. Enforcing layer-wise reasoning constraints while reducing training costs offers a promising approach to mitigate permutation-induced hallucinations.

Limitations

While this work demonstrates the effectiveness of Stable-RAG in mitigating permutation-induced hallucinations, it has several limitations that warrant further investigation.

First, our approach focuses on stabilizing reasoning at the final-layer representation level, without explicitly enforcing layer-wise reasoning path constraints throughout the model. Although our analysis reveals that permutation-induced divergence primarily emerges in the middle and higher layers, Stable-RAG does not directly regularize intermediate-layer reasoning trajectories. Incorporating explicit layer-wise constraints or trajectory-level alignment may further improve reasoning stability, but would require more fine-grained supervision or architectural modifications, which we leave for future work.

Second, Stable-RAG relies on spectral clustering over document-permuted hidden representations to estimate dominant reasoning modes and construct preference signals for DPO alignment. While this strategy reduces annotation cost by approximately threefold compared to exhaustive full-permutation decoding, it still incurs non-trivial computational and labeling overhead. More efficient clustering strategies, weak supervision signals, or fully unsupervised alignment objectives could further reduce annotation requirements and improve scalability. Exploring such cost-effective supervision mechanisms is an important direction for building more robust and practical RAG systems.

Ethical Considerations

While Stable-RAG aims to enhance the robustness and factual accuracy of RAG systems, several ethical considerations remain. First, although the method reduces hallucinations caused by document order, it cannot guarantee fully correct outputs; users should avoid over-reliance in high-stakes domains such as healthcare, law, or finance. Second, Stable-RAG relies on external documents for grounding, which may contain biases or errors, potentially propagating or amplifying such issues.

References

Amos Azaria and Tom Mitchell. 2023. [The internal state of an LLM knows when it’s lying](#). In *Findings of the Association for Computational Linguistics: EMNLP 2023*, pages 967–976, Singapore. Association for Computational Linguistics.

Jiangui Chen, Ruqing Zhang, Jiafeng Guo, Yixing Fan, and Xueqi Cheng. 2022. Gere: Generative evidence retrieval for fact verification. In *Proceedings of the 45th International ACM SIGIR Conference on Research and Development in Information Retrieval*, pages 2184–2189.

Yuhan Chen, Ang Lv, Ting-En Lin, Changyu Chen, Yuchuan Wu, Fei Huang, Yongbin Li, and Rui Yan. 2024. [Fortify the shortest stave in attention: Enhancing context awareness of large language models for effective tool use](#). In *Proceedings of the 62nd Annual Meeting of the Association for Computational Linguistics (Volume 1: Long Papers)*, pages 11160–11174, Bangkok, Thailand. Association for Computational Linguistics.

Florin Cuconasu, Giovanni Trappolini, Federico Siciliano, Simone Filice, Cesare Campagnano, Yoelle Maarek, Nicola Tonello, and Fabrizio Silvestri. 2024. The power of noise: Redefining retrieval for rag systems. In *Proceedings of the 47th International ACM SIGIR Conference on Research and Development in Information Retrieval*, pages 719–729.

Abhimanyu Dubey, Abhinav Jauhri, Abhinav Pandey, Abhishek Kadian, Ahmad Al-Dahle, Aiesha Letman, Akhil Mathur, Alan Schelten, Amy Yang, Angela Fan, and 1 others. 2024. The llama 3 herd of models. *arXiv e-prints*, pages arXiv–2407.

Wenqi Fan, Yujuan Ding, Liangbo Ning, Shijie Wang, Hengyun Li, Dawei Yin, Tat-Seng Chua, and Qing Li. 2024. A survey on rag meeting llms: Towards retrieval-augmented large language models. In *Proceedings of the 30th ACM SIGKDD conference on knowledge discovery and data mining*, pages 6491–6501.

Feiteng Fang, Yuelin Bai, Shiwen Ni, Min Yang, Xiaojun Chen, and Ruifeng Xu. 2024. [Enhancing noise robustness of retrieval-augmented language models with adaptive adversarial training](#). In *Proceedings of the 62nd Annual Meeting of the Association for Computational Linguistics (Volume 1: Long Papers)*, pages 10028–10039, Bangkok, Thailand. Association for Computational Linguistics.

Yunfan Gao, Yun Xiong, Xinyu Gao, Kangxiang Jia, Jinliu Pan, Yuxi Bi, Yixin Dai, Jiawei Sun, Haofen Wang, and Haofen Wang. 2023. Retrieval-augmented generation for large language models: A survey. *arXiv preprint arXiv:2312.10997*, 2(1).

Xiangming Gu, Tianyu Pang, Chao Du, Qian Liu, Fengzhuo Zhang, Cunxiao Du, Ye Wang, and Min Lin. When attention sink emerges in language models: An empirical view. In *The Thirteenth International Conference on Learning Representations*.

Cheng-Yu Hsieh, Yung-Sung Chuang, Chun-Liang Li, Zifeng Wang, Long Le, Abhishek Kumar, James Glass, Alexander Ratner, Chen-Yu Lee, Ranjay Krishna, and Tomas Pfister. 2024. [Found in the middle: Calibrating positional attention bias improves long](#)

- context utilization. In *Findings of the Association for Computational Linguistics: ACL 2024*, pages 14982–14995, Bangkok, Thailand. Association for Computational Linguistics.
- Edward J Hu, Yelong Shen, Phillip Wallis, Zeyuan Allen-Zhu, Yuanzhi Li, Shean Wang, Lu Wang, and Weizhu Chen. 2022. **LoRA: Low-rank adaptation of large language models**. In *International Conference on Learning Representations*.
- Qiushi Huang, Shuai Fu, Xubo Liu, Wenwu Wang, Tom Ko, Yu Zhang, and Lilian Tang. 2023. **Learning retrieval augmentation for personalized dialogue generation**. In *Proceedings of the 2023 Conference on Empirical Methods in Natural Language Processing*, pages 2523–2540, Singapore. Association for Computational Linguistics.
- Taeho Hwang, Sukmin Cho, Soyeong Jeong, Hoyun Song, SeungYoon Han, and Jong C. Park. 2025. **EXIT: Context-aware extractive compression for enhancing retrieval-augmented generation**. In *Findings of the Association for Computational Linguistics: ACL 2025*, pages 4895–4924, Vienna, Austria. Association for Computational Linguistics.
- Gautier Izacard, Mathilde Caron, Lucas Hosseini, Sebastian Riedel, Piotr Bojanowski, Armand Joulin, and Edouard Grave. 2021. Unsupervised dense information retrieval with contrastive learning. *arXiv preprint arXiv:2112.09118*.
- Mandar Joshi, Eunsol Choi, Daniel Weld, and Luke Zettlemoyer. 2017. **TriviaQA: A large scale distantly supervised challenge dataset for reading comprehension**. In *Proceedings of the 55th Annual Meeting of the Association for Computational Linguistics (Volume 1: Long Papers)*, pages 1601–1611, Vancouver, Canada. Association for Computational Linguistics.
- Vladimir Karpukhin, Barlas Oguz, Sewon Min, Patrick Lewis, Ledell Wu, Sergey Edunov, Danqi Chen, and Wen-tau Yih. 2020. **Dense passage retrieval for open-domain question answering**. In *Proceedings of the 2020 Conference on Empirical Methods in Natural Language Processing (EMNLP)*, pages 6769–6781, Online. Association for Computational Linguistics.
- Tom Kwiatkowski, Jennimaria Palomaki, Olivia Redfield, Michael Collins, Ankur Parikh, Chris Alberti, Danielle Epstein, Illia Polosukhin, Jacob Devlin, Kenton Lee, Kristina Toutanova, Llion Jones, Matthew Kelcey, Ming-Wei Chang, Andrew M. Dai, Jakob Uszkoreit, Quoc Le, and Slav Petrov. 2019. **Natural questions: A benchmark for question answering research**. *Transactions of the Association for Computational Linguistics*, 7:452–466.
- Sungjae Lee, Hoyoung Kim, Jeongyeon Hwang, Eunhyeok Park, and Jungseul Ok. 2025. **Efficient latent semantic clustering for scaling test-time computation of LLMs**. In *Findings of the Association for Computational Linguistics: EMNLP 2025*, pages 24126–24144, Suzhou, China. Association for Computational Linguistics.
- Patrick Lewis, Ethan Perez, Aleksandra Piktus, Fabio Petroni, Vladimir Karpukhin, Naman Goyal, Heinrich Küttler, Mike Lewis, Wen-tau Yih, Tim Rocktäschel, and 1 others. 2020. Retrieval-augmented generation for knowledge-intensive nlp tasks. *Advances in neural information processing systems*, 33:9459–9474.
- Yucheng Li, Bo Dong, Frank Guerin, and Chenghua Lin. 2023. **Compressing context to enhance inference efficiency of large language models**. In *Proceedings of the 2023 Conference on Empirical Methods in Natural Language Processing*, pages 6342–6353, Singapore. Association for Computational Linguistics.
- Zhonghao Li, Xuming Hu, Aiwei Liu, Kening Zheng, Sirui Huang, and Hui Xiong. 2024. **Refiner: Restructure retrieved content efficiently to advance question-answering capabilities**. In *Findings of the Association for Computational Linguistics: EMNLP 2024*, pages 8548–8572, Miami, Florida, USA. Association for Computational Linguistics.
- Zhenwen Liang, Ruosen Li, Yujun Zhou, Linfeng Song, Dian Yu, Xinya Du, Haitao Mi, and Dong Yu. 2025. Clue: Non-parametric verification from experience via hidden-state clustering. *arXiv preprint arXiv:2510.01591*.
- Hongzhan Lin, Ang Lv, Yang Song, Hengshu Zhu, Rui Yan, and 1 others. 2024. Mixture of in-context experts enhance llms’ long context awareness. *Advances in Neural Information Processing Systems*, 37:79573–79596.
- Andrew Ng, Michael Jordan, and Yair Weiss. 2001. On spectral clustering: Analysis and an algorithm. *Advances in neural information processing systems*, 14.
- Shiyu Ni, Keping Bi, Jiafeng Guo, Lulu Yu, Baolong Bi, and Xueqi Cheng. 2025. **Towards fully exploiting LLM internal states to enhance knowledge boundary perception**. In *Proceedings of the 63rd Annual Meeting of the Association for Computational Linguistics (Volume 1: Long Papers)*, pages 24315–24329, Vienna, Austria. Association for Computational Linguistics.
- Han Peng, Jinhao Jiang, Zican Dong, Xin Zhao, and Lei Fang. 2025. **CAFE: Retrieval head-based coarse-to-fine information seeking to enhance multi-document QA capability**. In *Proceedings of the 2025 Conference on Empirical Methods in Natural Language Processing*, pages 12977–12989, Suzhou, China. Association for Computational Linguistics.
- Alexander Peysakhovich and Adam Lerer. 2023. Attention sorting combats recency bias in long context language models. *arXiv preprint arXiv:2310.01427*.
- Ofir Press, Noah A Smith, and Mike Lewis. 2021. Train short, test long: Attention with linear biases enables input length extrapolation. *arXiv preprint arXiv:2108.12409*.

- Rafael Rafailov, Archit Sharma, Eric Mitchell, Christopher D Manning, Stefano Ermon, and Chelsea Finn. 2023. Direct preference optimization: Your language model is secretly a reward model. *Advances in neural information processing systems*, 36:53728–53741.
- Jianlin Su, Murtadha Ahmed, Yu Lu, Shengfeng Pan, Wen Bo, and Yunfeng Liu. 2024. Roformer: Enhanced transformer with rotary position embedding. *Neurocomputing*, 568:127063.
- Ulrike Von Luxburg. 2007. A tutorial on spectral clustering. *Statistics and computing*, 17(4):395–416.
- Leandro von Werra, Younes Belkada, Lewis Tunstall, Edward Beeching, Tristan Thrush, Nathan Lambert, Shengyi Huang, Kashif Rasul, and Quentin Galouédec. 2020. Trl: Transformer reinforcement learning. <https://github.com/huggingface/trl>.
- Shuting Wang, Xin Yu, Mang Wang, Weipeng Chen, Yutao Zhu, and Zhicheng Dou. 2025a. RichRAG: Crafting rich responses for multi-faceted queries in retrieval-augmented generation. In *Proceedings of the 31st International Conference on Computational Linguistics*, pages 11317–11333, Abu Dhabi, UAE. Association for Computational Linguistics.
- Yifei Wang, Feng Xiong, Yong Wang, Linjing Li, Xiangxiang Chu, and Daniel Dajun Zeng. 2025b. POSITION BIAS MITIGATES POSITION BIAS: Mitigate position bias through inter-position knowledge distillation. In *Proceedings of the 2025 Conference on Empirical Methods in Natural Language Processing*, pages 1495–1512, Suzhou, China. Association for Computational Linguistics.
- Thomas Wolf, Lysandre Debut, Victor Sanh, Julien Chaumond, Clement Delangue, Anthony Moi, Pierric Cistac, Tim Rault, Remi Louf, Morgan Funtowicz, Joe Davison, Sam Shleifer, Patrick von Platen, Clara Ma, Yacine Jernite, Julien Plu, Canwen Xu, Teven Le Scao, Sylvain Gugger, and 3 others. 2020. Transformers: State-of-the-art natural language processing. In *Proceedings of the 2020 Conference on Empirical Methods in Natural Language Processing: System Demonstrations*, pages 38–45, Online. Association for Computational Linguistics.
- Guangxuan Xiao, Yuandong Tian, Beidi Chen, Song Han, and Mike Lewis. Efficient streaming language models with attention sinks. In *The Twelfth International Conference on Learning Representations*.
- Fangyuan Xu, Weijia Shi, and Eunsol Choi. 2024. Re-comp: Improving retrieval-augmented lms with context compression and selective augmentation. In *The Twelfth International Conference on Learning Representations*.
- An Yang, Anfeng Li, Baosong Yang, Beichen Zhang, Binyuan Hui, Bo Zheng, Bowen Yu, Chang Gao, Chengen Huang, Chenxu Lv, and 1 others. 2025. Qwen3 technical report. *arXiv preprint arXiv:2505.09388*.
- Zhilin Yang, Peng Qi, Saizheng Zhang, Yoshua Bengio, William Cohen, Ruslan Salakhutdinov, and Christopher D. Manning. 2018. HotpotQA: A dataset for diverse, explainable multi-hop question answering. In *EMNLP*, pages 2369–2380, Brussels, Belgium. Association for Computational Linguistics.
- Ori Yoran, Tomer Wolfson, Ori Ram, and Jonathan Berant. 2024. Making retrieval-augmented language models robust to irrelevant context. In *The Twelfth International Conference on Learning Representations*.
- Hanning Zhang, Shizhe Diao, Yong Lin, Yi Fung, Qing Lian, Xingyao Wang, Yangyi Chen, Heng Ji, and Tong Zhang. 2024a. R-tuning: Instructing large language models to say ‘I don’t know’. In *Proceedings of the 2024 Conference of the North American Chapter of the Association for Computational Linguistics: Human Language Technologies (Volume 1: Long Papers)*, pages 7113–7139, Mexico City, Mexico. Association for Computational Linguistics.
- Qianchi Zhang, Hainan Zhang, Liang Pang, Hongwei Zheng, Yongxin Tong, and Zhiming Zheng. 2025. Less is more: Compact clue selection for efficient retrieval-augmented generation reasoning. *arXiv preprint arXiv:2502.11811*.
- Qianchi Zhang, Hainan Zhang, Liang Pang, Hongwei Zheng, and Zhiming Zheng. 2024b. Adacomp: Extractive context compression with adaptive predictor for retrieval-augmented large language models. *arXiv preprint arXiv:2409.01579*.
- Zhenyu Zhang, Runjin Chen, Shiwei Liu, Zhewei Yao, Olatunji Ruwase, Beidi Chen, Xiaoxia Wu, Zhangyang Wang, and 1 others. 2024c. Found in the middle: How language models use long contexts better via plug-and-play positional encoding. *Advances in Neural Information Processing Systems*, 37:60755–60775.
- Yujia Zhou, Yan Liu, Xiaoxi Li, Jiajie Jin, Hongjin Qian, Zheng Liu, Chaozhuo Li, Zhicheng Dou, Tsung-Yi Ho, and Philip S Yu. 2024. Trustworthiness in retrieval-augmented generation systems: A survey. *arXiv preprint arXiv:2409.10102*.
- Junda Zhu, Lingyong Yan, Haibo Shi, Dawei Yin, and Lei Sha. 2024a. ATM: Adversarial tuning multi-agent system makes a robust retrieval-augmented generator. In *Proceedings of the 2024 Conference on Empirical Methods in Natural Language Processing*, pages 10902–10919, Miami, Florida, USA. Association for Computational Linguistics.
- Kun Zhu, Xiaocheng Feng, Xiyuan Du, Yuxuan Gu, Weijiang Yu, Haotian Wang, Qianglong Chen, Zheng Chu, Jingchang Chen, and Bing Qin. 2024b. An information bottleneck perspective for effective noise filtering on retrieval-augmented generation. In *Proceedings of the 62nd Annual Meeting of the Association for Computational Linguistics (Volume 1: Long Papers)*, pages 1044–1069, Bangkok, Thailand. Association for Computational Linguistics.

Appendix

Contents

| | | |
|----------|--|-----------|
| A | Implementation Details | 12 |
| A.1 | Datasets | 12 |
| A.2 | Baseline Details | 12 |
| A.3 | Training Details | 13 |
| A.4 | Prompts | 13 |
| B | Mathematical Derivations | 13 |
| B.1 | Spectral Clustering on Hidden States | 13 |
| B.2 | Similarity Graph and Adjacency Matrix | 13 |
| B.3 | Degree Matrix and Normalized Laplacian | 14 |
| B.4 | Eigen-decomposition and Determining Cluster Number | 14 |
| B.5 | Spectral Embedding and Clustering | 14 |
| C | More Experimental Results | 14 |
| C.1 | Permutation Sensitivity in Qwen3 Models | 14 |
| C.2 | Structural Instability Across Model Families | 14 |
| C.3 | Visualization of Layer-wise Hidden States | 15 |
| C.4 | Cross-Retriever Transferability | 15 |
| C.5 | Original vs. Shuffled Order | 16 |

A Implementation Details

A.1 Datasets

We conduct experiments on three widely used QA datasets that cover both single-hop and multi-hop question-answering scenarios. Table 6 summarizes the key statistics of these datasets. Specifically, **NQ** (Kwiatkowski et al., 2019) and **TriviaQA** (Joshi et al., 2017) are representative single-hop datasets, where each question can typically be answered using information from a single passage retrieved from the corpus. These datasets primarily evaluate a model’s ability to locate and extract factual evidence efficiently. In contrast, **HotpotQA** (Yang et al., 2018) is a challenging multi-hop dataset that requires integrating and reasoning over multiple pieces of evidence distributed across different documents to derive the final answer. This dataset is particularly useful for testing

a model’s reasoning and compositional understanding capabilities. Together, these datasets provide a comprehensive benchmark for evaluating both the retrieval quality and reasoning robustness of our proposed method under diverse task settings.

| Dataset | Type | # Train | # Dev | # Test |
|----------|------------|---------|-------|--------|
| NQ | single-hop | 79.1k | 8.7k | 3.6k |
| TriviaQA | single-hop | 78.7k | 11.3k | 8.8k |
| HotpotQA | multi-hop | 88.9k | 5.6k | 5.6k |

Table 6: Statistics for the datasets.

A.2 Baseline Details

We compare Stable-RAG with the following baseline strategies. To ensure a fair comparison, all methods are evaluated on the same test set and retrieved set.

Vanilla Methods. (i) *Direct Generation*. This baseline relies solely on the generator’s parametric knowledge to produce answers without consulting any retrieved documents. (ii) *Vanilla RAG* (Lewis et al., 2020). This baseline concatenates all retrieved documents as model input without any additional processing. (iii) *Vanilla SFT*. We implement vanilla SFT following Zhang et al. (2024a). For each training example, this baseline uses the gold answer as the training label if it appears in the retrieved documents; otherwise, it assigns “*I don’t know*” as the training label to guide the model to abstain when the necessary information is missing.

Robust RAG. (i) *RetRobust* (Yoran et al., 2024). This baseline improves retrieval-augmented QA models by filtering out irrelevant retrieved passages and fine-tuning the model on a mix of relevant and irrelevant contexts, enabling it to leverage relevant information while remaining robust to irrelevant content. (ii) *ATM* (Zhu et al., 2024a). This baseline optimizes a retrieval-augmented Generator using an Adversarial Tuning Multi-agent system, where an auxiliary Attacker agent iteratively steers the Generator to better discriminate useful documents from noisy or fabricated ones, improving robustness and performance on knowledge-intensive question answering tasks. (iii) *RAAT* (Fang et al., 2024). This baseline dynamically adjusts the model’s learning process in response to various types of retrieval noise through adaptive adversarial training, while employing multi-task learning to enable the model to internally recognize and handle noisy contexts,

thereby improving robustness and answer quality in retrieval-augmented generation.

Positional Bias. (i) *Pos2Distill* (Wang et al., 2025b). This baseline mitigates positional bias in long-context tasks by transferring knowledge from advantageous positions to less favorable ones through position-to-position knowledge distillation. (ii) *Ms-PoE* (Zhang et al., 2024c). This baseline uses Multi-scale Positional Encoding to mitigate the "lost-in-the-middle" issue in LLMs by rescaling positional indices and assigning different scaling ratios to attention heads, enabling multi-scale context fusion without fine-tuning or extra overhead.

A.3 Training Details

We use LLaMA3-8B-Instruct¹ (Dubey et al., 2024) and Qwen3-8B² (Yang et al., 2025) as backbone models for experiments. We implement our DPO training pipeline using the HuggingFace Transformers (Wolf et al., 2020) and TRL libraries (von Werra et al., 2020), incorporating PEFT LoRA (Hu et al., 2022) for parameter-efficient fine-tuning. Both the base model and reference model are initialized from pre-trained checkpoints, with the reference model kept in evaluation mode to provide stable policy targets during training. Each dataset is randomly shuffled and split into 85% training and 15% validation samples, with a maximum of 18,000 samples per dataset to control computational overhead. To guarantee reproducible results, we use a fixed random seed with a value of 42. LoRA is applied to all projection layers, including query, key, value, output, gate, up, and down projections, with rank $r = 128$, alpha = 128, dropout = 0 and no additional bias terms. The DPO configuration uses a per-device batch size of 2 with gradient accumulation of 8, a learning rate of 5×10^{-6} , a linear warmup ratio of 0.1, and a preference scaling hyperparameter β of 0.4. We train LLaMA-3-8B-Instruct for a single epoch and Qwen3-8B for two epochs on two NVIDIA RTX PRO 6000 GPUs, with each epoch taking roughly two hours. After training, the fine-tuned models and tokenizers are saved for downstream evaluation.

Notably, we set the generation temperature to 0.01 during data construction and inference, effectively approximating greedy decoding to ensure that output variations primarily reflect document-

¹<https://huggingface.co/meta-llama/Meta-Llama-3-8B-Instruct>

²<https://huggingface.co/Qwen/Qwen3-8B>

```
<system>
You are a helpful, respectful, and honest
assistant. Answer the question with couple
of words using the provided documents.
For example: Question: What is the capital
of France? Output: Paris.
</system>
<user>
Question: {query}
Documents:
Doc1: {Document 1}
Doc2: {Document 2}
.....
</user>
```

Table 7: Prompt for the backbone LLMs.

order sensitivity rather than sampling randomness.

A.4 Prompts

We adopt a system-user style prompting scheme to guide the backbone LLMs to generate concise, document-grounded answers, as presented in Table 7.

B Mathematical Derivations

We employ spectral clustering on hidden states to identify dominant reasoning modes across permutations of retrieved documents. Compared with conventional clustering methods, spectral clustering captures the global structure of the hidden state space. This enables Stable-RAG to robustly group similar reasoning behaviors, reduce noise from spurious variations, and improve the consistency of preference signals used for DPO alignment.

B.1 Spectral Clustering on Hidden States

Spectral clustering is applied to the hidden states matrix

$$H = [h^{(1)}, h^{(2)}, \dots, h^{(N)}]^T \in \mathbb{R}^{N \times d}$$

to adaptively determine the number of clusters and capture the global structure of the hidden state space, where each cluster corresponds to a latent reasoning mode (Lee et al., 2025).

B.2 Similarity Graph and Adjacency Matrix

We construct a weighted similarity graph $G = (V, E)$ where each node corresponds to a hidden

state $h^{(i)}$ and edges encode pairwise similarities. The adjacency matrix $A \in \mathbb{R}^{N \times N}$ is computed as the exponential of the cosine distance:

$$A_{ij} = \exp\left(-\frac{h^{(i)} \cdot h^{(j)}}{\|h^{(i)}\| \|h^{(j)}\|}\right),$$

where σ is a hyperparameter controlling sensitivity.

B.3 Degree Matrix and Normalized Laplacian

The degree matrix D is a diagonal matrix with entries

$$D_{ii} = \sum_{j=1}^N A_{ij}.$$

The normalized graph Laplacian is

$$L = I - D^{-1/2} A D^{-1/2},$$

where I is the identity matrix.

B.4 Eigen-decomposition and Determining Cluster Number

Let $\lambda_1 \leq \dots \leq \lambda_N$ be the eigenvalues of L . Define the consecutive eigengaps as

$$\text{gap}_i = \lambda_{i+1} - \lambda_i.$$

The number of clusters K is set adaptively as

$$K = \max\left(2, \left(\arg \max_i \text{gap}_i\right) + 1\right),$$

ensuring clear separation between latent reasoning modes following standard practice (Ng et al., 2001; Von Luxburg, 2007).

B.5 Spectral Embedding and Clustering

We then compute the first K eigenvectors of L , normalize each row to unit length, and apply standard clustering to assign each hidden state $h^{(i)}$ to one of the clusters

$$C_1, C_2, \dots, C_K,$$

exactly following the procedure described in the main text.

C More Experimental Results

C.1 Permutation Sensitivity in Qwen3 Models

We further investigate whether document-order sensitivity generalizes to different model families by reporting Perturbation Success Rate (PSR) results on the Qwen3 series. Following the same evaluation protocol as in Figure 1, we fix the gold document in different positions and measure the proportion of document-order perturbations that lead to

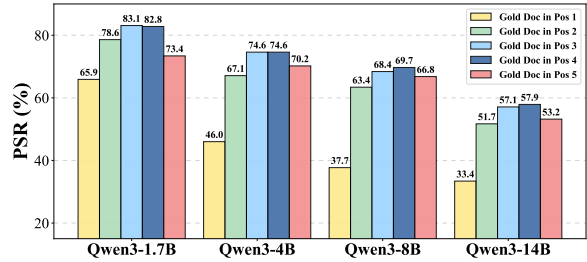


Figure 8: **Perturbation Success Rate (PSR)** on the NQ test set across different Qwen3 models. PSR is computed as the proportion of successful document-order perturbations to produce hallucination results among 1000 randomly sampled instances, with the gold document fixed in the different positions.

hallucinated outputs over 1,000 randomly sampled instances on the NQ test set.

Figure 8 compares the PSR trends of the Qwen3 models with those observed in the LLaMA-3 Instruct series. Overall, Qwen3 models exhibit clear document-order sensitivity across all model sizes. When the gold document is placed at early positions, the PSR is relatively low, indicating stronger robustness to document-order perturbations. However, as the gold document is shifted to later positions, PSR increases substantially, suggesting a higher likelihood of hallucinations induced purely by document reordering.

We observe a consistent monotonic pattern across Qwen3 variants: PSR generally rises from Top-1 to Top-3 or Top-4 and slightly saturates or declines afterward. This behavior closely mirrors the trends observed in LLaMA-3 models, despite differences in model architecture and pretraining data. Moreover, smaller Qwen3 models tend to exhibit higher sensitivity to document order changes, while larger models demonstrate comparatively improved robustness, though the issue remains non-negligible even at larger scales.

These results indicate that document-order sensitivity is not specific to a particular model family but rather a general phenomenon shared across contemporary large language models. The consistent patterns across both LLaMA-3 and Qwen3 series further motivate the need for order-robust RAG methods.

C.2 Structural Instability Across Model Families

We provide additional visualizations of the structural instability in internal reasoning dynamics for both the LLaMA-3 and Qwen3 model families as

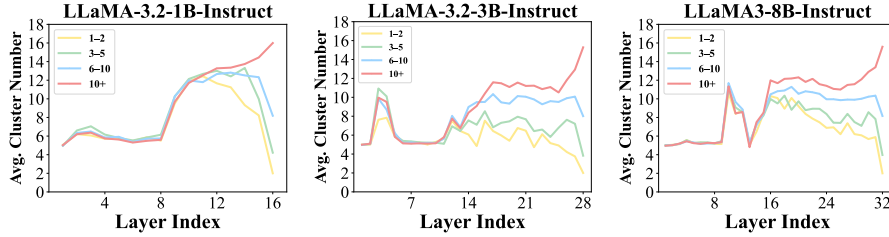


Figure 9: Hidden-state clustering behaviors across layers for LLaMA3 series models on the NQ train set with DPR retriever, using 1,000 random sampled instances. Different colored lines indicate the number of clusters of final reasoning states produced by the LLM under all $5! (= 120)$ permutations of the Top-5 retrieved documents (e.g., the green line indicates 3–5 cluster states).

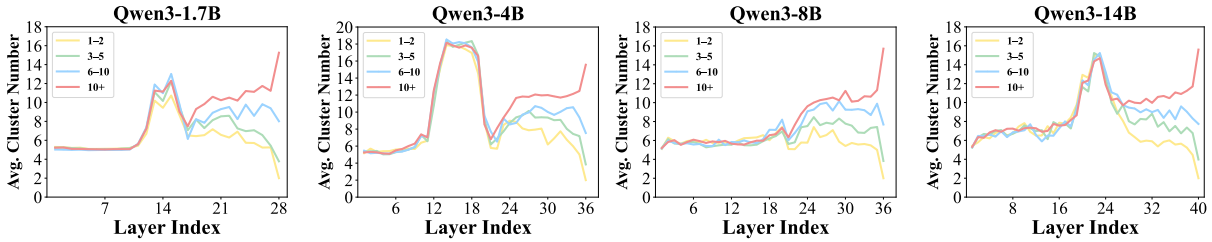


Figure 10: Hidden-state clustering behaviors across layers for Qwen3 series models on the HotpotQA train set with Contriever retriever, using 1,000 random sampled instances. Different colored lines indicate the number of clusters of final reasoning states produced by the LLM under all $5! (= 120)$ permutations of the Top-5 retrieved documents (e.g., the green line indicates 3–5 cluster states).

shown in Figure 9 and Figure 10. Following the same analysis protocol as in the main paper, we examine how document permutations induce divergence in hidden representations across different model layers.

Despite differences in architecture, scale, and pretraining data, both model families exhibit highly consistent patterns of structural instability. Specifically, hidden representations in shallow layers remain relatively concentrated under document permutations, while substantial divergence emerges in the middle layers and becomes more pronounced in higher layers. Moreover, samples exhibiting higher permutation sensitivity consistently show greater representational divergence than stable samples, with this effect primarily localized to the middle layers.

These observations suggest that permutation sensitivity originates from a shared structural instability in the reasoning dynamics of large language models rather than from model-specific design choices. The consistent trends observed across both LLaMA-3 and Qwen3 families further support the necessity of addressing structural instability to improve the robustness of RAG systems.

C.3 Visualization of Layer-wise Hidden States

Figure 12 shows LLaMA3-8B-Instruct on NQ using the Contriever retriever, illustrating the hidden state evolution across all layers for a selected example. Figure 13 displays Qwen3-8B on HotpotQA dataset using Contriever dataset, showing the layer-wise progression of hidden states for a representative sample. In both cases, shallow layers exhibit mixed clusters with points corresponding to different answers interleaved, while deeper layers form increasingly well-separated clusters according to the final answers. These visualizations reinforce that the structural evolution of reasoning trajectories, as observed in the main experiments, is consistent across multiple models and datasets.

C.4 Cross-Retriever Transferability

As reported in Section 5.3, we evaluated transfer from DPR to Contriever. Here, we additionally test transfer from Contriever to DPR, as shown in Figure 11. Both experiments confirm that Stable-RAG consistently improves answer consistency and reduces permutation-induced variance across different retrievers, demonstrating robust cross-retriever generalization.

| Method | NQ | | | TriviaQA | | | HotpotQA | | |
|-------------------|--------------|--------------|-------------|--------------|--------------|-------------|--------------|--------------|-------------|
| | Original | Shuffled | Drop | Original | Shuffled | Drop | Original | Shuffled | Drop |
| Vanilla SFT | 42.10 | 36.43 | 5.67 | 55.52 | 53.19 | 2.33 | 27.25 | 22.48 | 4.77 |
| RetRobust | 41.82 | 38.06 | 3.76 | 64.85 | 62.86 | 1.99 | 31.46 | 29.18 | 2.28 |
| ATM | 43.75 | 42.47 | 1.28 | 66.37 | 63.60 | 2.77 | 34.36 | 32.46 | 1.90 |
| RAAT | 42.33 | 40.54 | 1.79 | 65.58 | 62.19 | 3.39 | 33.58 | 29.75 | 3.83 |
| Pos2Distill | 44.58 | 43.63 | 0.95 | 64.13 | 63.57 | 0.56 | 32.73 | 32.09 | 0.64 |
| Ms-PoE | 40.32 | 39.17 | 1.15 | 64.21 | 62.96 | 1.25 | 30.17 | 29.14 | 1.03 |
| Ours (Stable-RAG) | 48.14 | 47.23 | 0.91 | 72.05 | 71.76 | 0.29 | 38.91 | 37.50 | 1.41 |

Table 8: Performance comparison of LLaMA3-8B-Instruct with Contriever retriever under original and shuffled document order across three QA datasets. We report SubEM for evaluation.

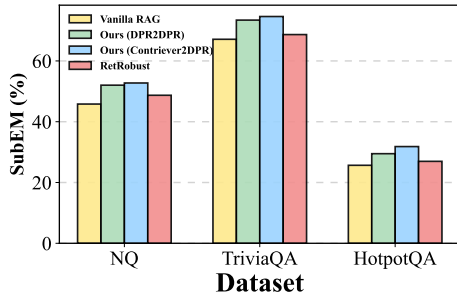


Figure 11: Cross-Retriever Transferability.

C.5 Original vs. Shuffled Order

Table 8 presents a comparison of answer performance under the original document order and a randomly shuffled order across three QA datasets. Our method achieves the highest SubEM scores in both original and shuffled conditions across all datasets, demonstrating its robustness to retrieval order permutations and its ability to maintain stable answer consistency.

Question: what is the liquid in a magic 8 ball? Correct Answer(s): Alcohol.
● Alcohol. ● Water.

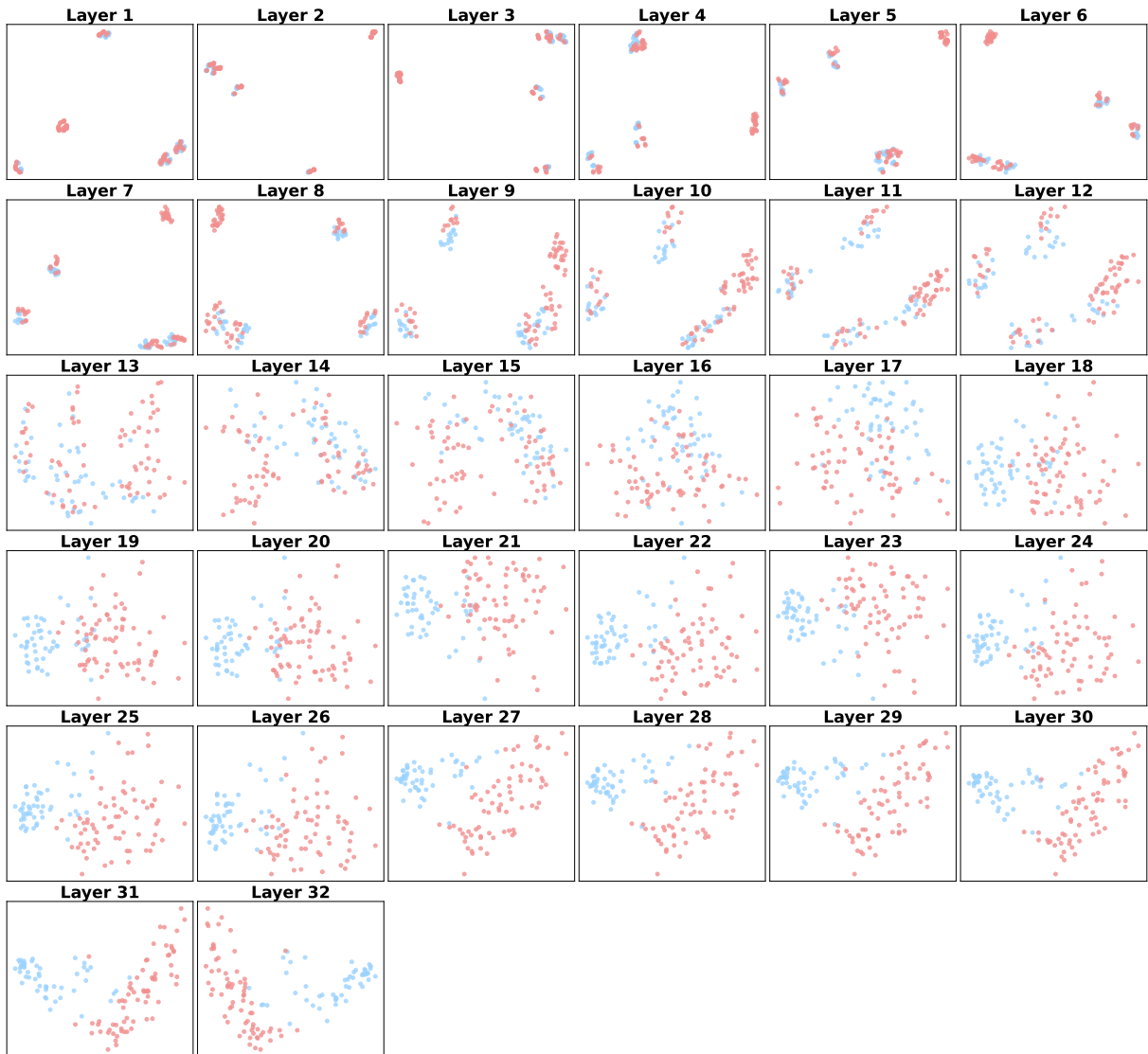


Figure 12: 2D PCA visualization of hidden state representations across all layers in LLaMA3-8B-Instruct for a single example. Each point corresponds to a document order, and its color represents the model's final answer.

Question: Which band has more members, Muse or The Raconteurs? Correct Answer(s): The Raconteurs.
● Muse has more members. ● Muse. ● The Raconteurs.

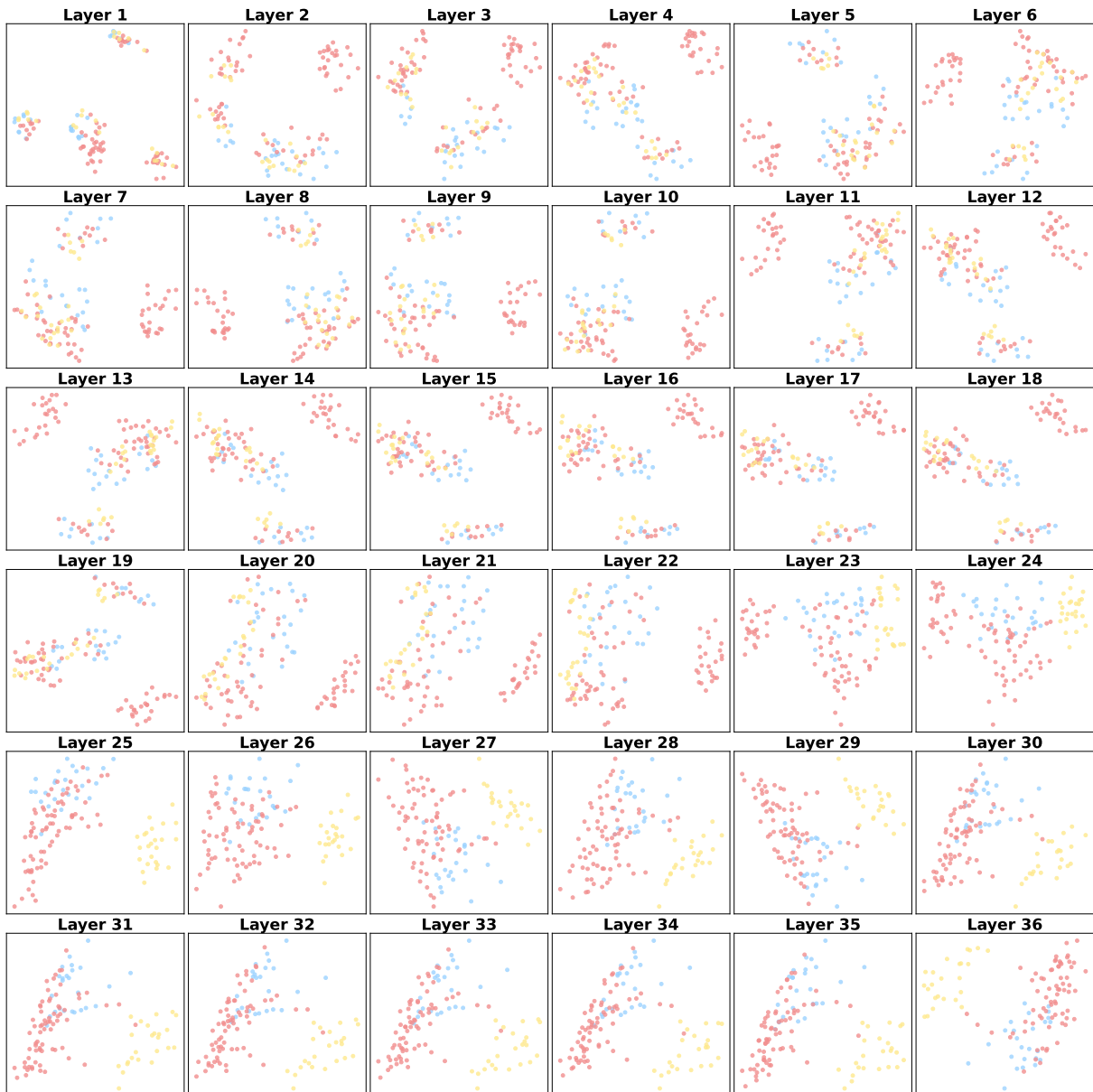


Figure 13: 2D PCA visualization of hidden state representations across all layers in Qwen3-8B for a single example. Each point corresponds to a document order, and its color represents the model's final answer.